RESEARCH ARTICLE

DOI: 10.5935/0946-5448.20240038

International Tinnitus Journal. 2024;28(2):261-277

Development of a Temporary Threshold Shift Model of Chronic Noise-Induced Tinnitus with Evidence of Altered Auditory Signaling Pathway Inhibition

Xiaoping Du[1],
Jianzhong Lu[1],
Zachary Yokell[1],
Qunfeng Cai[1],
Weihua Cheng[1],
Don Nakmali[1],
Wei Li[1],
Richard D Kopke[1],
Matthew B. West[1]

ABSTRACT

Our laboratory has developed a unique rodent model of chronic noise-induced tinnitus (NIT) that results from an acoustic overexposure trauma associated with multi-frequency temporary threshold shifts (TTSs) during the acute phase of the injury, which are resolved to near baseline levels by four weeks post-exposure (i.e. < 5 dB of permanent threshold shifts). The resultant multi-frequency manifestations of NIT evidenced by the startle reflex inhibition test in this model coincide with significant reductions in the sizes of outer hair cell (OHC) efferent termini across the same tonotopic frequency range, as well as significant changes in tinnitus-related biomarkers in the auditory system as objective evidence for the NIT. Notably, this TTS NIT model does not induce any significant HC loss and only presents with afferent ribbon synapse loss in the high tonotopic frequency region outside of the putative histopathological area of emphasis for tinnitus, creating a unique opportunity to study the functional consequences of reduced efferent signaling and tinnitus-related biomarker expression in the auditory system on the development and specification of a chronic tinnitus percept without confounding variables, such as HC loss or widespread de-afferentation that add considerable complexity to the relevant electrophysiological evaluations. Significant positive correlation between expression of glutamate receptor 2 in the central auditory system and tinnitus score in this TTS NIT model provides evidence that altered glutamate responsivity in the CNS is linked to the development of NIT. We believe that this TTS NIT model can serve as a strong candidate for targeted tinnitus-related pharmaceutical studies.

Keywords: Acoustic trauma, Acoustic startle reflex test, Rodent, Biomarkers, Plasticity, Cochlear efferent terminals.

Hough Ear Institute, Oklahoma City, Oklahoma, United States of America

***Send correspondence to**
Matthew B West
Hough Ear Institute, 3400 NW 56th St. Oklahoma City, OK 73112, United States of America, E-mail: mwest@houghear.org

Paper submitted on Dec 02, 2024; and Accepted on Dec 26, 2024

INTRODUCTION

Tinnitus, the perception of a phantom sound in the absence of an external acoustic stimulation, has been linked to common sequelae of acoustic overexposures[1]. Tinnitus occurs in 15-20% of the population and is one of the most prevalent service-related disabilities in the U.S. military[2,3]. The military represents an especially high-risk population for noise-induced cochlear traumas and comorbidities, such as tinnitus, with up to 600,000 military personnel exposed to high noise environments. However, tinnitus is also highly prevalent and relevant to the general population, as work and recreational acoustic overexposures remain prevalent in our society[4]. The National Institute for Occupational Safety and Health published a report in 2007 which addressed the prevalence of hearing loss and tinnitus. They found that 7% of U.S. workers never exposed to hazardous occupational noise levels had hearing difficulty; 5% had tinnitus; and 2% had both conditions. However, among workers who had been exposed to hazardous occupational noise levels, the prevalences were elevated to 23%, 15%, and 9%, respectively[5]. Most people with tinnitus (~ 60%) have some level of hearing loss; however, some 13 million Americans report tinnitus without hearing loss[4, 6]. In fact, cochlear synaptopathy without hearing loss may be sufficient for the genesis of tinnitus[7-11] and may explain why many individuals have tinnitus without Permanent Threshold Shifts (PTS). In light of its high prevalence and potentially distressing impact on quality of life, there is an urgent need to objectively characterize and develop new therapeutic targets and clinical signatures for effectively diagnosing this auditory disorder and mitigating its adverse neurological impact.

It is now widely appreciated that the loss of cochlear afferent Ribbon Synapses (RSs) on sound-transducing inner hair cells (IHCs) represents a major factor underlying all forms of Sensorineural Hearing Loss (SNHL)[12]. In the mammalian cochlea, IHCs are innervated by 12-20 RSs which coalesce and relay peripheral auditory information to the brain through specialized neurons within the cochlear spiral ganglion. Studies in several species of mammals indicate that a subset of IHC RSs with high thresholds and low spontaneous firing rates are particularly susceptible to loss from noise, aging, and ototoxic insults[13]. These findings correlate with human temporal bone studies in which widespread auditory nerve fiber and synapse loss have been documented as early as the third decade and become increasingly prevalent with age[13]. Liberman and colleagues have hypothesized that partial de-afferentation of IHCs is widespread in human ears across a range of acquired SNHL etiologies, with or without overt hearing loss[12]. Although emphasis has been placed on de-afferentation of IHCs as an etiological catalyst for tinnitus, more recent studies argue that differences in cochlear efferent innervation status may also play a critical role in driving the tinnitus percept[14, 15]. There is also conflicting data regarding the role that sound-amplifying Outer Hair Cell (OHC) efferent innervation status and plasticity might play in this disorder[16, 17]. As a result, there is a need to better elucidate and distinguish the impact of efferent synaptopathy and plasticity in the etiology of tinnitus.

The descending cochlear efferent system, which consists of lateral and medial olivocochlear efferent neural relays that project axons from the brainstem to the cochlea, provides feedback inhibition that modulates hearing sensitivity and protects against excitotoxicity. Medial efferent nerve relays primarily originate from the contralateral medial olivary complex and innervate OHCs, modulating their electromotility and hearing sensitivity and the noise/signal ratio[18]. The lateral olivocochlear nerve fibers primarily originate from the ipsilateral lateral olivary complex and innervate auditory nerve fiber dendrites near IHCs[19]. Recent clinical evidence suggests that the efferent system, particularly the medial efferent pathway, may play a role in tinnitus generation and maintenance[20-23]. However, the functional status of the efferent system in the context of Noise-Induced Tinnitus (NIT) has not been unambiguously examined in animal models.

An imbalance between inhibition and excitation in the central auditory system is another proposed mechanism that may drive or contribute to the maintenance of tinnitus. One leading hypothesis is that inhibition, through impaired γ-aminobutyric acid (GABA) synaptic transmission, becomes compromised in this context, which has led to the rationale that the use of GABAA receptor potentiators (GABAkines) might be a viable approach for treating this disorder[24]. This concept is supported by the fact that both mRNA transcripts and membrane-bound protein expression of GABAA receptor units are reduced in the Auditory Cortex (AC) following an acoustic trauma[25, 26]. Moreover, noise exposures that only induce Temporary Threshold Shifts (TTS) have, nonetheless, also been shown to evoke decreases in GABAergic inhibition in the Dorsal Cochlear Nucleus (DCN) of animals with behavioral evidence of tinnitus[27, 28]. This central disinhibition hypothesis of tinnitus is complemented by the recognition that up-regulation of the excitatory neurotransmitter, glutamate (Glu), is likely to also play a key play a role in perpetuating the disorder[29]. Indeed, magnetic resonance spectroscopy evaluations have shown that, in a rat model of NIT, Glu is, indeed, elevated in the DCN and AC[30]. Thus, glutamate receptor antagonists have also been proposed as potential therapeutics for treating tinnitus[31, 32]. In the mammalian CNS, alpha-amino-3-hydroxy-5-methyl-4-isooxazole-propionic acid (AMPA)-type glutamate receptors are the primary modulators of fast-excitatory synaptic transmission, and changes to their tetrameric subunit compositions fine-tune their affinity for Glu and synaptic plasticity, making them logical targets for tailored therapeutic intervention[33, 34]. Despite the apparent conceptual cohesion of these putative therapeutic approaches, considerable heterogeneity in neurotransmission patterns have been measured among neurons in the central auditory pathway in response to peripheral damage, suggesting that highly-complex patterns of evoked neuroplasticity are possible,

which high-resolution studies are just now beginning to untangle[35, 36].

In the current study, we have developed a unique rodent TTS model of chronic NIT to study the functional consequences of reduced afferent and/or efferent signaling, and tinnitus-related biomarker expression in the auditory system on the development and specification of a chronic tinnitus percept in the absence of canonical confounding variables, such as HC loss or significant PTSs.

MATERIALS & METHODS

Animals

Male Sprague Dawley (SD) rats, aged 1–3 months, were used in histological, behavioral and physiological procedures on NIT. Rats weighing 250–300 g were purchased from Charles River Laboratories (Wilmington, MA) and were maintained on a normal day/night cycle at 21°C with free access to food and water. They were provided a 1-week acclimation period prior to experimental procedures. For this study, rats were divided into two groups: (1) normal hearing group (naïve control group, NC) not subjected to noise exposure, and (2) noise exposure group, in which animals underwent noise exposure. All rats were administered intraperitoneal saline injections (5 mL/kg, twice/day) initiated 24h after noise exposure for a total of five doses to mimic handling/hydration impact of potential acute treatment regimens[37]. The noise exposure group was further divided into two subgroups after prepulse inhibition (PPI) of the acoustic startle reflex test: the noise-exposed with tinnitus (N/T+) group and the noise-exposed without tinnitus (N/T-) group. All procedures regarding the use and handling of animals were approved by the Institutional Animal Care and Use Committee of the University of Oklahoma Health Sciences Center.

Noise Exposure

Under anesthesia (ketamine 80 mg/kg + xylazine 10 mg/kg, intraperitoneal injection), rats were exposed to an octave-band noise (OBN) of 8–16 kHz with a center frequency of 11.3 kHz at 108 dB sound pressure level (SPL) for two hours in a uniform sound intensity noise field in a sound reverberant chamber, where rats were placed on an acoustically-transparent wired platform. The OBN was generated by Tucker-Davis Technologies (TDT), Inc.'s App, RPvdsEx, running on the TDT apparatus, RP2.1 Enhanced Real-Time Processor, amplified (3600 Watts) with a PLX-3602 Power Amplifier (QSC Audio Products Inc.) and delivered to a JBL 2446H driver/JBL 3860a Bi Radial Horn assembly (QSC Audio Products, Inc.). The noise intensity and noise profile were analyzed and monitored by a B&K 4189 ½" microphone, and a B&K 3160 Front End Processor preamplifier, using B&K's Pulse Labshop App (Bruel and Kjaer Instrument, Inc.). The sound intensity in the noise field was found to be varied less than 1.00 dB SPL. OBN from 106-114 dB had been tested in a group of rats in a pilot experiment, and 108 dB OBN that induced TTS only was used in the following experiments.

Auditory Brainstem Responses (ABRs)

ABRs were measured bilaterally, testing each ear separately in a sound booth (Industrial Acoustics Company). For testing, animals were anesthetized with ketamine (80 mg/kg) and xylazine (10 mg/kg) via intraperitoneal injection, while basal body temperature was maintained with a servo heating pad. Stimulus generation and data acquisition were accomplished with a TDT RX6 workstation running TDT BioSigRP software. Acoustic stimuli were tone bursts of alternating polarity with a 5-ms plateau and 0.5-ms $\cos^2$ rise-fall envelope at frequencies of 4, 8, 16, and 32 kHz. Tone bursts were presented monaurally in free-field mode using a TDT MF1 speaker, which was placed 10 cm lateral to the pinna and was driven by a TDT stereo power amplifier. ABRs were recorded using sub-dermal needle electrodes located at the vertex (active), the ipsilateral mastoid (reference), and the contralateral mastoid (ground), where the responses were amplified 10,000×, band-pass filtered from 0.3 to 3 kHz, and averaged across 512 repetitions at a rate of 21/s. Sound intensities were varied in 5-dB steps up and down to identify ABR thresholds. The threshold was defined as the lowest dB stimulus level that yielded a repeatable, clearly discernible, waveform by visual analysis of stacked waveforms from the highest to lowest SPL.

Quantification of cochlear HCs

Rats were euthanized 4 weeks after noise exposure. The entire basal membrane from each cochlea was micro-dissected out and blocked in 1% bovine serum albumin (fraction V, BSA) in 0.1 M phosphate-buffered saline (PBS, pH 7.2) for at least one hour at room temperature (RT). Myosin VIIa immunolabeling of HCs (1:1000, Proteus Biosciences, Ramona, CA) and phalloidin labeling of stereocilia were performed and the number of IHCs and OHCs was counted using a fluorescence microscope (Olympus BX51, Japan), according to published protocols[37].

PPI of the acoustic startle reflex test

Gap and acoustic PPI test sessions were adapted from Lu et al.[37] and were based upon the ability of the acoustic startle reflex to be reduced when preceded either by a silent gap in a constant acoustic background or by an acoustic burst in a quiet background. Briefly, the StartleMonitor/AuxAmp II system (Kinder Scientific, LLC) was used for the behavioral testing, where animals were tested inside of a sound-attenuating box with two loudspeakers mounted in its ceiling and with a piezoelectric transducer platform positioned on its floor. The prepulse and background sounds were presented through one speaker (XT25TG30-04, Vifa), while startle stimuli were presented through the other speaker (CTS KSN-1005, Powerline). Attached to the animal holder, the piezoelectric transducer provided a measure of the startle force applied by the animal. The startle stimuli

were 50-ms broadband noise bursts (0 ms rise-fall) at an intensity of 107 dB SPL. Here, there were two modalities of prepulses for PPI tests—i.e., for acoustic PPI tests, the prepulse was a bandpass noise burst, whereas for gap-PPI tests, the prepulse was a silent gap in an otherwise continuous carrier. With an envelope of 50 ms in length featuring 1.0-ms ramps that occurred 100 ms prior to the startle stimulus, the acoustic prepulse and the gap carrier were both filtered noise (one-third octave bandpass with a 48 dB/octave roll-off) with frequencies centered at 9.3, 16, 20, and 24 kHz, each at an intensity of 60 dB SPL. The test session began with a 2-min acclimation period followed by three startle-only trials to habituate the startle response to a stable baseline. For the remainder of the session, a mixture of additional startle-only ("baseline") trials in quiet or with continuous frequency-specific background sounds, along with acoustic or gap-PPI trials, was conducted in a counter-balanced fashion. The startle amplitude was determined by the peak force in newtons following the onset of the startle stimulus. The PPI was defined as a fractional reduction of startle (i.e., the ratio of startle amplitude with vs. without prepulse), thus, a value of 1 meant no effect of the prepulse, and a value of 0 meant complete inhibition of startle. In this study, we used the tinnitus index score as a metric, which is calculated by subtracting the acoustic PPI from the gap PPI, to determine the presence of a tinnitus percept in animals. Higher scores are indicative of tinnitus-like deficits in processing silent gap cues. The test procedure was performed on four consecutive days, and the useful data collection was implemented during the last two days. The measurements of these two-day tests were averaged for each animal. Animals were excluded from the PPI dataset if they met the criterion, i.e., "baseline" startle responses in a quiet background were < 3 standard deviations above the average highest activity level happening before the onset of startle. Extreme values in the dataset were removed when identified as outliers by applying Grubb's method.

Collection of cochlear tissues for RS evaluations

Animals used for RS counts were decapitated under deep anesthesia with ketamine and xylazine at successive time points between 24 hours and 4 weeks post-noise exposure (i.e. 24h, 72h, 1w, and 4w). Cochleae were quickly micro-dissected out in cold PBS. Round and oval windows were opened, and a hole was made in the apical portion of each cochlea. Four percent formaldehyde solution in PBS was perfused into the cochlea for tissue fixation. The cochleae were placed in the same fixative for an additional 10 min at 4 °C. After fixation, cochleae were further dissected in PBS and then blocked in PBS containing 1% Triton X-100 and 5% normal horse serum for one hour before immunolabeling with a combination of rabbit anti-GluR2/3 antibody (Millipore Bioscience, catalog # AB1506, 1:100) and mouse anti-C-terminal binding protein 2 antibody (CtBP2, BD Transduction Laboratories, catalog # 612044, 1:200) for 20 h at 37 °C. The tissues were rinsed with PBS and incubated with Alexa Fluor488 chicken anti-rabbit (1:1000, Life Technologies, Co., Grand Island, NY) for one hour at 37 °C, and then rinsed with PBS and incubated with Alexa Fluor488 goat anti-chicken antibody (1:1000, Life Technologies, Co., Grand Island, NY) and Alexa Fluor568 goat anti-mouse antibody (1:1000, Life Technologies, Co., Grand Island, NY) for another hour at 37 °C. The tissues were counterstained with DAPI (4′,6-diamidino2-phenylindole) for 10 min at RT and then mounted on slides with anti-fade medium. Six cochlear frequency locations, 2, 4, 8, 16, 32, and 48 kHz, were selected for image collection as confocal z-stacks. Images were acquired in a 1024×1024 pixel frame with 0.5 μm steps in the z plane, using a Zeiss LSM-710 confocal microscope (Carl Zeiss Microimaging, LLC, NY). Each stack contained six to nine IHCs with entire sets of RSs. 3-D morphometry was processed using Amira 3D software (FEI, Burlington, MA). The presynaptic ribbons (red channel) and postsynaptic densities (green channel) were identified by segmentation, quantified and tracked in the z-dimension, and divided by the total number of IHCs in the microscopic field, according to previously published methods[38, 39].

OHC efferent terminus immunolabeling, counting and size measurement

Animals used for efferent terminus evaluations were euthanized and intracardially-perfused with saline followed by 4% paraformaldehyde in PBS at successive time points between 24 hours and 4 weeks post-noise exposure (i.e. 24h, 72h, 1w, and 4w). The basal membrane with the organ of Corti from each cochlea was micro-dissected out and blocked with 1% BSA and 1% normal goat serum in PBS for 1 hour and then incubated with goat anti-choline acetyltransferase (ChAT) antibody (1:100, NOVUS Biologicals, Littleton, CO) and rabbit anti-myosin VIIa antibody (1:1000, Proteus Biosciences, Ramona, CA) overnight at RT. After washing with PBS, the basal membrane was incubated with appropriate secondary antibodies (1:1000, Life Technologies, Co., Grand Island, NY) for two hours at RT followed by DAPI labeling and mounting in anti-fade medium. The whole cochlea was photographed with a fluorescence microscope. Cochlear length was measured and frequency was computed using a custom ImageJ plug-in (https://masseyeandear.org/research/otolaryngology/eaton-peabody-laboratories/histology-core). Changes in olivocochlear efferent innervation were examined by confocal microscopy (Zeiss LSM-710 confocal microscope, Carl Zeiss Microimaging, LLC, NY), then quantified, using NIH ImageJ software, by measuring the number of ChAT silhouettes per OHC and the size of each silhouette in maximum projections of confocal z-stacks across the 9.3-22 kHz regions for each cochlea.

Biomarker study in the peripheral and central auditory system

To study tinnitus-related biomarker expression on the development and specification of a chronic tinnitus percept, a total of 19 rats were used for brain and

cochlear sectioning and subsequent immunohistological evaluations. Animals in each experimental group (5–7 rats/group) were euthanized and intracardially-perfused with saline followed by 4% paraformaldehyde in PBS at four weeks post-noise exposure. Brains, brainstems, and cochleae were removed and post-fixed in the same fixative (one week for brain tissues and overnight for cochleae), washed with PBS three times, and then stored in PBS at 4˚ C.

For vanilloid receptor 1 (VR1) or oligomeric Tau (T22) immunostaining in the spiral ganglion (sg), fixed cochleae were washed with PBS and then decalcified for two weeks in 10% EDTA with solution changes two times each week. Cochleae were then dehydrated, embedded in paraffin, and sectioned in a paramodiolar plane at a thickness of 6 μm. Every 10th section was mounted on a slide (total of 10 slides per cochlea), and the mounted cochlear sections were processed for immunohistochemical analyses. Cochlear sections were de-paraffinized in xylene and re-hydrated in serial concentrations of ethanol and distilled water. The sections were blocked with 1% BSA and 1% normal goat serum in PBS for 1 hour and then incubated with rabbit anti-VR1 antibody (1:1000, EMD Millipore, Billerica, MA, catalog# AB5370) or rabbit anti-oligomeric Tau serum (T22, 1:100, kindly gifted from Dr. Rakez Kayed at University of Texas Medical Branch) overnight at RT. After washing with PBS containing 0.2% Triton X-100 (PBS/T), either biotinylated goat anti-rabbit IgG or horse anti-mouse IgG (1:200, Vector Laboratories, Inc. Burlingame, CA) was applied to the slides for one hour at RT, and Vectastain ABC and DAB kits (Vector Laboratories, Inc. Burlingame, CA) were used for the immunolabeling visualization. Images were collected with a BX51 Olympus microscope from the spiral ganglion in the basal and middle turns of all sections on each slide. The number of VR1- or T22-positive neurons was quantified using ImageJ software. The percentage of VR1- or T22-positive neurons in the SG (positive stained/ total number of neurons x 100%) was calculated and statistically analyzed, as described previously[37].

The brain and brainstem from each animal were cryoprotected in 30% sucrose in PBS at 4˚C until the tissue settled to the bottom of the container. Brain tissues were then embedded in Tissue-Tek (Sakura Finetek USA Inc. Torrance, CA) and serially sectioned in a coronal plane with a Thermo Cryotome (Thermo Fisher Scientific, Inc. Waltham, MA) at 20 μm. One section out of every ten from each brain and brainstem was mounted onto a gelatin pre-coated slide (total of 10 slides for each brainstem and 20 slides for each brain). The distance between two adjacent sections on each slide was about 200 μm.

For immunohistological staining, brain sections were blocked in 1% BSA and either 1% normal horse serum or 1% normal goat serum in PBS/T. Blocked and permeabilized sections were then incubated with either rabbit anti-$GABA_AR$-α1 antibody (1:500, EMD Millipore, Billerica, MA, catalog# 06–868), mouse anti-glutamate receptor 2 antibody (GluR2, 1:100, EMD Millipore, Billerica, MA, catalog# MAB 397), or rabbit anti-oligomeric Tau serum (T22, 1;100, kindly gifted from Dr. Rakez Kayed at University of Texas Medical Branch) overnight at RT followed by visualization processing as detailed above. Immuno-positive cells exhibited a brown reaction product at the sites of the target epitopes. Methyl green was used for nuclear counter-staining. Negative controls were prepared by omitting the primary antibodies.

For quantitative evaluations, images were collected with a BX51 Olympus microscope. In the brainstem, DCN images were collected from the medial third (medial), the middle third (middle) and the lateral third (lateral) sections[40, 41]. In the AC, images were collected from all layers (two images to cover all layers on one section). In the hippocampus, images were collected from the polymorph layer of the dentate gyrus (PoDG). A modified two-dimensional quantification method was employed to count immuno-positive cells in these nuclei or regions[41, 42]. The total number of immuno-positive cells within each image was quantified using ImageJ software (National Institutes of Health) by a technician who was unaware of the identity of the samples on each slide. Only dark brown-stained cells were counted. The density of each biomarker-positive cell (number of positive cells/mm2) was calculated and statistically analyzed.

Statistical Analyses

To determine the perception of tinnitus, a 95% Confidence Interval (CI) for the average tinnitus index score was constructed for each test frequency based on the dataset from the companion control group. Noise-exposed rats with tinnitus index scores above the 95% CI were deemed different from not-exposed control subjects and were considered to have tinnitus at that given test frequency. ANOVA was used to compare the means of multiple groups. When the global F-test revealed the existence of an overall statistically-significant difference, a Tukey's HSD for all-pairwise comparisons or a Dunnett's test for multiple-to-one comparisons was chosen as a follow-up to ANOVA. To analyze an association of tinnitus behavior with various quantitative biomarker measurements, a Pearson correlation coefficient was computed as a measure, where the bootstrapping approach was employed for hypothesis testing. To handle count data for histological analysis, Poisson regression was used to model count variables, where a p-value was obtained by likelihood ratio test. Unless otherwise specified, statistical tests were performed using R software (version 4.3.2). SPSS 14.0 Version for Windows was used for quantitative histological biomarker analysis in an overall ANOVA.

RESULTS

TTS model development

An initial cohort of time-synchronized naïve controls and noise-exposed (8-16 kHz OBN, 2h, 108 dB) SD rats were contemporaneously carried through a regimen of ABR testing upon enrollment (baseline) and at time equivalents

corresponding to 24h and 4w post-noise exposure to track the changes in ABR threshold sensitivity over time. Thirty-six (36) total SD rats were carried through this enrollment and testing regimen, with 18 rats exposed to noise and 18 rats serving as naïve controls. In the noise-exposed group, ABR threshold (T) levels measured at 24h and 4w post-noise at each test frequency were used to calculate threshold shifts (TSs) in comparison to baseline ABR thresholds measured for each animal prior entry into the study (i.e. $T_{terminal} - T_{baseline}$, dB). Relative to the mean thresholds for the companion naïve controls measured at 4 weeks after exposure, noise-exposed subjects showed a consistent and significant temporary threshold elevation at 24 hours (i.e., ~26.6 dB, the mean difference between the conditions of exposure and control after collapsing across all 4 frequencies, $F(2,50) = 182.26$, $P < 0.001$ by a Dunnett's test following a two-way mixed ANOVA), which fully recovered in the test frequency region at 4 weeks ($p > 0.05$ **Figure 1A**). These results demonstrated that the noise exposure paradigm induced a significant TTS that did not persist as a PTS (< 5dB on average at all test frequencies) at the terminal 4w test interval.

To determine the degree of HC loss induced by the TTS, the numbers of IHCs and OHCs were measured in the cochleae of the naïve controls and noise-exposed rats at 4 weeks post-noise exposure. Depict cytocochleograms (graphical summaries) of the mean % of IHC and OHC loss quantified along the tonotopic breadth (i.e. entire organ of Corti, OC) of cochleae from these test animals. No IHC or OHC loss was denoted across the tonotopic frequency regions that correspond to the test frequencies of interest for this study. Only slight (< 10%) OHC loss was measured at the extreme basal turn (i.e. > 45 kHz tonotopic frequency position) in the OC from the noise-exposed group, which was not significantly different from that measured in time-synchronized naïve controls, indicating that the TTS did not induce significant HC loss in this model (all $p > 0.05$) (**Figure 1B and C**).

Noise-induced TTS is sufficient for generating chronic tinnitus percept

Based on the desired electrophysiological and histological profiles measured in our TTS test cohorts, we repeated the noised exposure and testing regimen in a new cohort of SD rats with the goal of expanding our evaluation to include PPI testing and a broader array of histological evaluations. ABR procedures were performed preexposure and at four weeks after exposure on 30 rats for PTS, where 5 animals

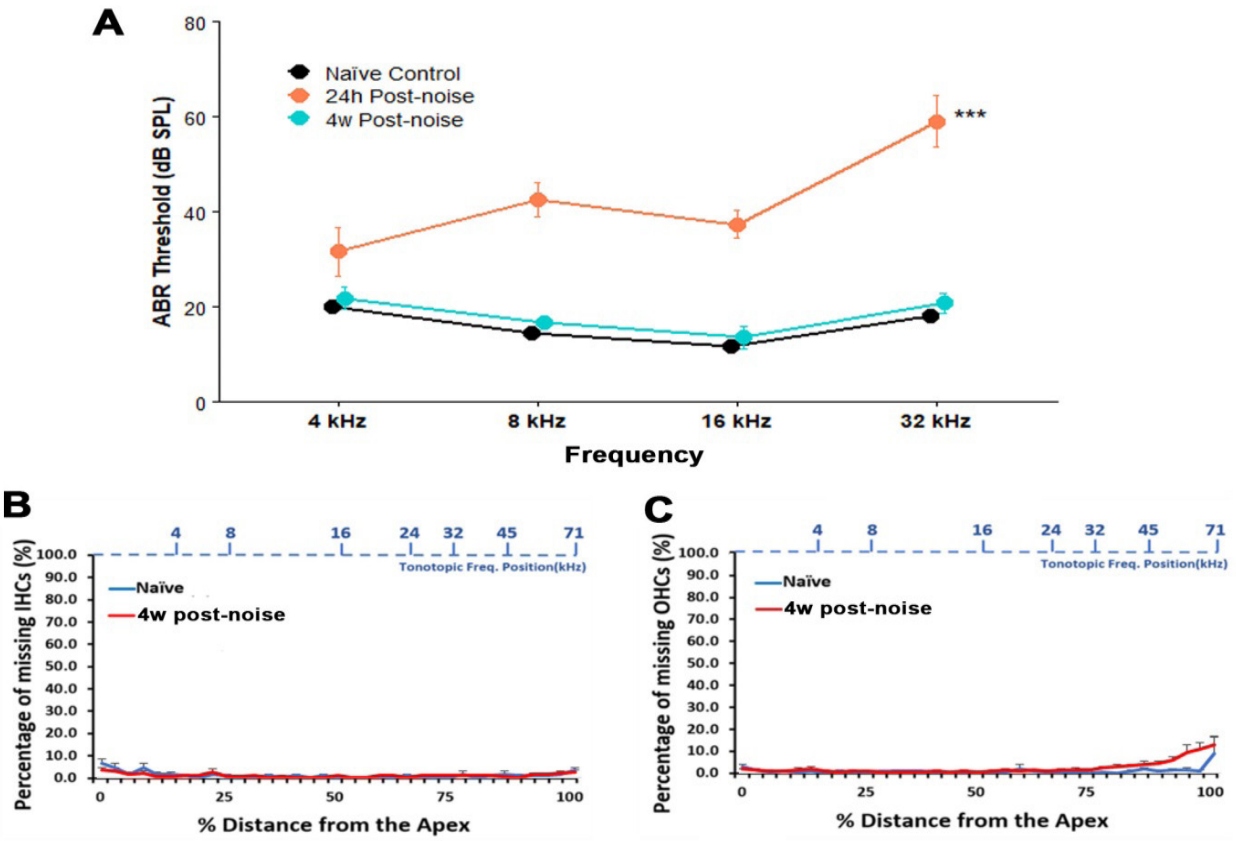

Figure 1: Noise exposure induces TTS and no HC loss in the cochlea. A. Temporary threshold elevation of about 27 dB ($p < 0.001$) with a full recovery to baseline (or preexposure) levels ($p > 0.05$) over time. Mean ABR thresholds (±SEMs) are shown at any given test frequency for the control group and the exposure group, each having 18 cases. *** $p < 0.001$ indicates a significant simple main effect of exposure at 24 hours. Quantification of IHCs (B) and OHCs (C) in the cochleae 4 weeks after noise exposure. There was no significant cochlear HC loss in the noise exposure group ($n = 14$) compared to the NC group ($n = 6$, all $p > 0.05$).

were randomly selected and tested at 24 h after exposure to confirm replication of the TTS. The noise exposure caused ~28.25 dB of TTS across frequencies ($F(1,4) = 127.37$, $P < 0.001$ by two-way repeated measures ANOVA)(**Figure 2A**); however, with time, this TTS was once-again resolved to near preexposure levels when testing was repeated 4w thereafter (PTS across frequencies = 4.025dB)(**Figure 2B**), although the statistical analysis yielded a significant result ($F(1,30) = 30.36$, $P < 0.001$ by two-way repeated measures ANOVA).

To test for noise-induced tinnitus-like behavior, we performed the PPI testing paradigm on the 30 noise-exposed rats at four weeks post-exposure as an assay for the presence of a tinnitus percept. The gap-PPI deficits among Noise-Exposed (NE) rats, compared with the normal behavioral score measured among 34 time-synchronized companion controls, showed that 20 animals out of the 30 NE rats developed tinnitus, at one or more test frequencies, resulting in an overall tinnitus incidence of 67%. Figure 3A shows tinnitus index scores for each NE rat at 9.3, 16, 20 and 24 kHz, wherein, for each frequency targeted, these animals with scores exceeding the 95% CI of the control group are hypothesized to have spectrally restricted tinnitus. According to data aggregated by the frequency variable, the frequency-specific incidence of tinnitus percepts has a wide variation in tinnitus tones (or pitches) demonstrating a wide tinnitus spectrum induced by this TTS model (**Figure 3B**).

High frequency RS loss in the cochlea of the TTS model

To study IHC RSs in the TTS model, IHC RS densities were evaluated at different time points after noise exposure. Reductions in IHC RS densities were rapid (24 hours after noise exposure) and permanent (no recovery at four weeks after noise exposure) in this TTS model at high tonotopic frequency positions of 32 and 45.2 kHz (all $p < 0.001$)(**Figure 4A**). However, IHC RS densities were not significantly changed at middle and low tonotopic positions (i.e. at frequencies of 22.6 kHz or **Figure 4A**).

To study IHC RSs in the TTS tinnitus model, IHC RS densities were evaluated in rats with or without tinnitus. Four weeks after noise exposure, the TTS model induced significant synaptopathy among IHC RSs at high tonotopic frequency positions (32 kHz and 45.2 kHz, $p < 0.01$ or 0.001) while no difference was observed between rats with or without tinnitus (all $p > 0.05$) (**Figure 4B**), indicating that RS loss induced by the TTS model was seemingly unrelated to tinnitus development.

Reduction of OHC efferent terminal sizes in the cochlea of the TTS model

To study OHC efferent termini in the TTS model, we measured OHC efferent terminal sizes and numbers in

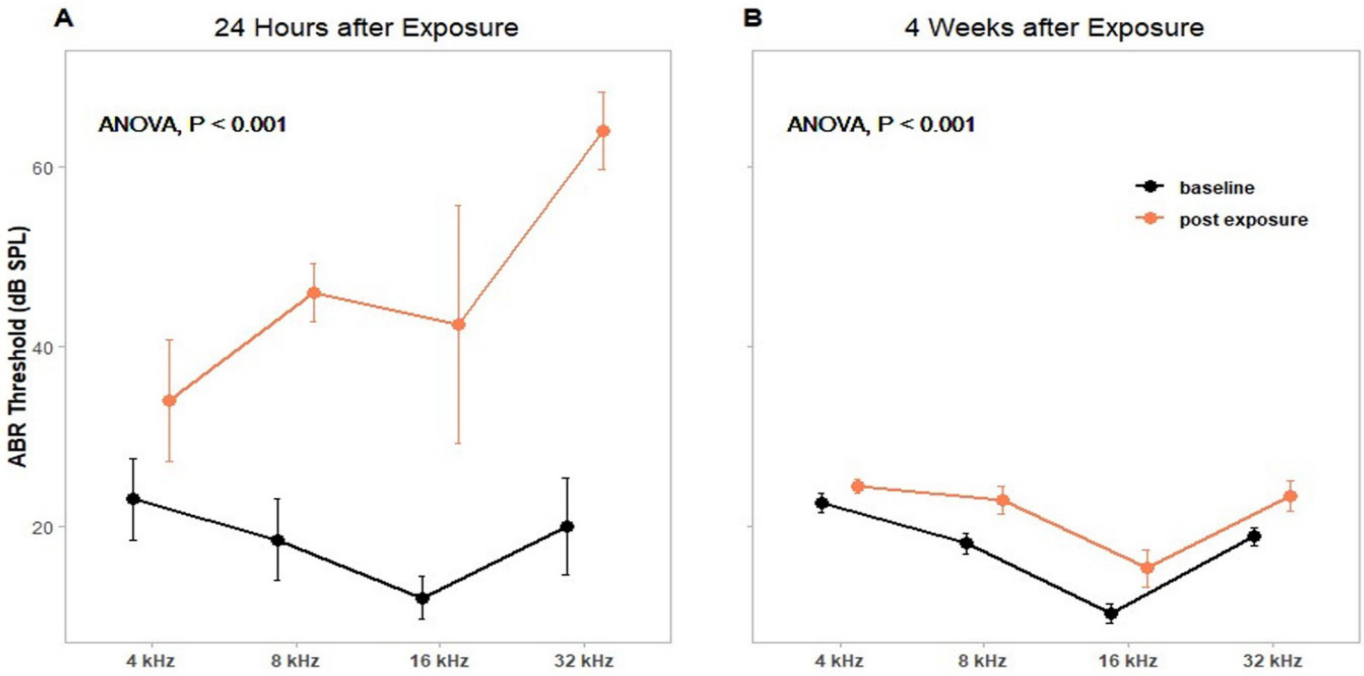

Figure 2: Noise exposure induces a temporary threshold elevation of about 28 dB ($p < 0.001$) in the ABR with recovery to near baseline (or preexposure) levels (PTS across frequencies = 4.025dB, $p < 0.001$) over time. Mean ABR thresholds (±SEMs) were measured 24 h (A) and 4 weeks (B), respectively, post exposure. The group size was n = 5 for "24 Hours after Exposure" (A) and n= 30 for "4 Weeks after Exposure" (B). P values by ANOVAs represent the main effect of the factor time after collapsing across all four levels of the factor frequency. Color key in B applies to both panels.

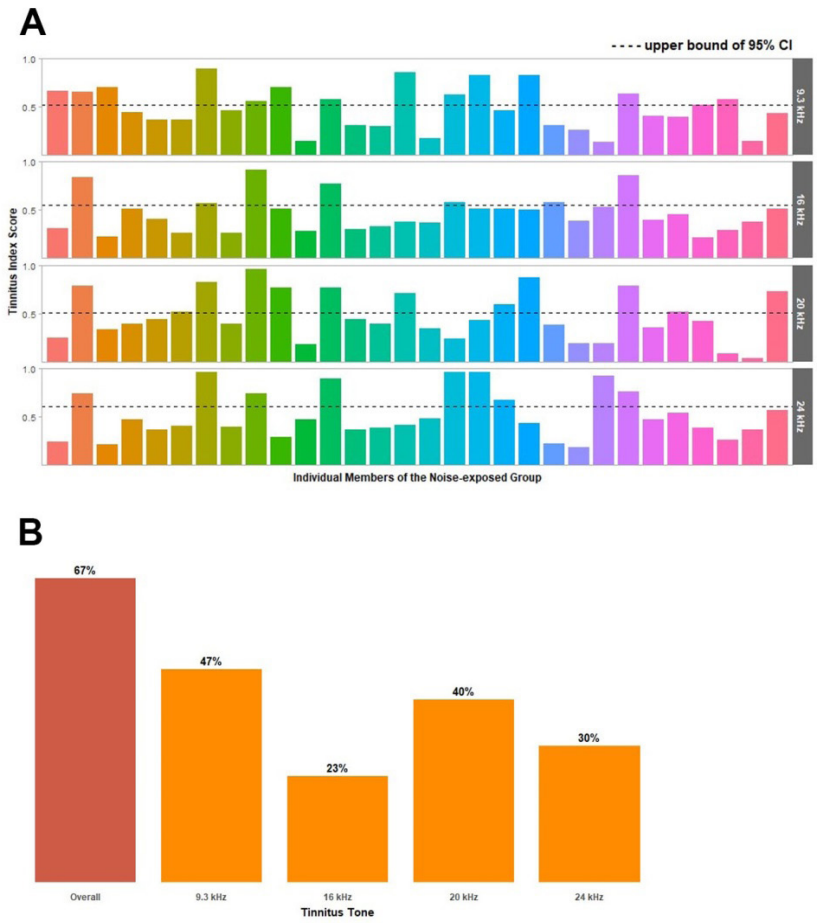

Figure 3: Tinnitus index scores 4 weeks after noise exposure. A. Between 0 and 1 individual tinnitus index scores are distributed by test frequencies for each subject. Each small bar represents a different subject. Subjects with index scores greater than the upper bound of 95% CI for the control group are considered to have tinnitus at that given frequency. B. In NE rats, the incidence of tinnitus percepts is manifested in a frequency-dependent way. Tinnitus tones (or pitches) are defined as test frequencies at which tinnitus index scores exceed the 95% CI for the companion not-exposed control group. Noise-induced tinnitus percepts are characterized by a wide frequency range of tinnitus tones. Data were obtained at 4 weeks after exposure from n = 30 cases.

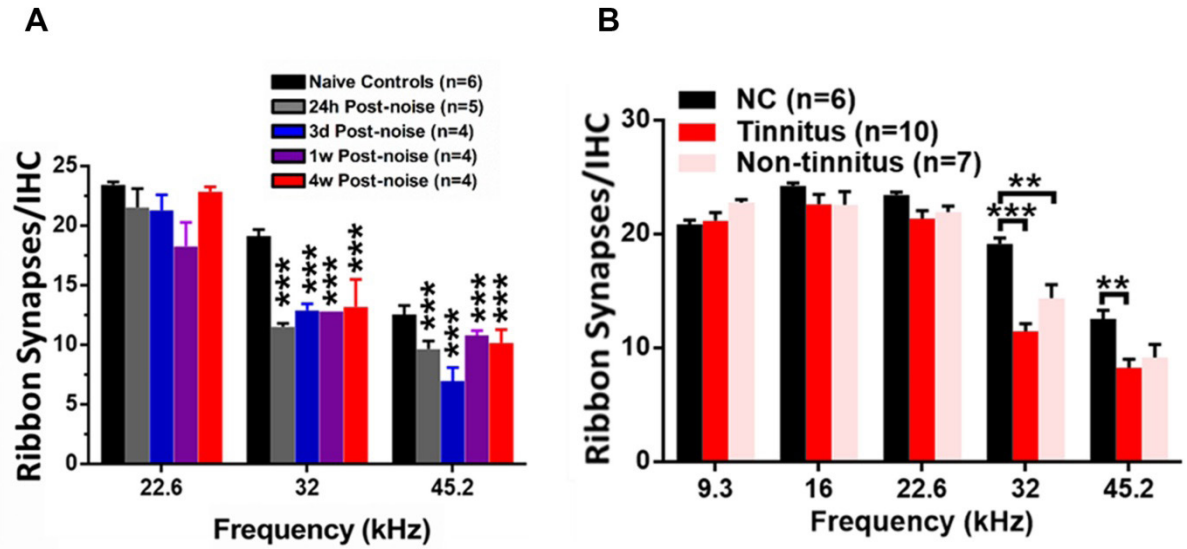

Figure 4: TTS model induced IHC RS loss in the cochlea. A. Reductions in IHC RS densities were rapid (24 hours after noise exposure) and permanent (4 weeks after noise exposure) in this TTS model at high tonotopic frequency positions (32 and 45.2 KHz, all $p < 0.001$). B. Four weeks after noise exposure the TTS model induced significant synaptopathy among IHC RSs at high tonotopic frequency positions in all NE rats (32 and 45.2 KHz, $p < 0.01$ or 0.001) while no difference was observed between rats with and without tinnitus (all $p > 0.05$).

the cochleae of rats at successive time points (1 day to 4 weeks) after noise exposure (**Figure 5A & B**). In naïve control rats, one to six medial efferent termini were counted on each OHC, while lateral efferent termini on IHCs were much smaller, more numerous and densely packed (data not shown). The average number of efferent termini per OHC was 1.79 at 9.3 KHz, 2.28 at 16 KHz, 2.43 at 20 KHz and 2.41 at 22 KHz. The number of efferent silhouettes under each OHC was not significantly changed at any time point (24 hours to 4 weeks) after noise exposure compared the NC group (all $p > 0.05$).

However, the sizes of ChAT silhouette areas were significantly and rapidly (i.e. within 24 hours) reduced after noise exposure. Reductions in silhouette size reached peak at three days after noise exposure and totally (i.e. in the 9.3 kHz region) or partially (i.e. in the 16 and 20 kHz regions) recovered 1 and 4 weeks after noise exposure. However, the reduction was permanent in the high frequency region (i.e. 22 kHz), with no measurable recovery 4 weeks after noise exposure **(Figure 5C)**.

We then measured OHC efferent terminal sizes and numbers in cochleae of rats with or without tinnitus at four weeks after noise exposure. Average silhouette areas were significantly reduced in the N/T+ and the N/T- groups compared to the NC group at tonotopic positions of 9.3, 16, 20 and 22 kHz (all $p < 0.001$). The N/T+ group had significantly smaller OHC ChAT silhouettes compared to the N/T- group at 16, 20, and 22 kHz (all $p < 0.001$, **Figure 5D**). These results indicate that the reduced sizes of efferent termini were tinnitus-related. However, the total number of efferent silhouettes under each OHC was not significantly reduced in the N/T+ and the N/T- groups compared to the NC group (all $p > 0.05$).

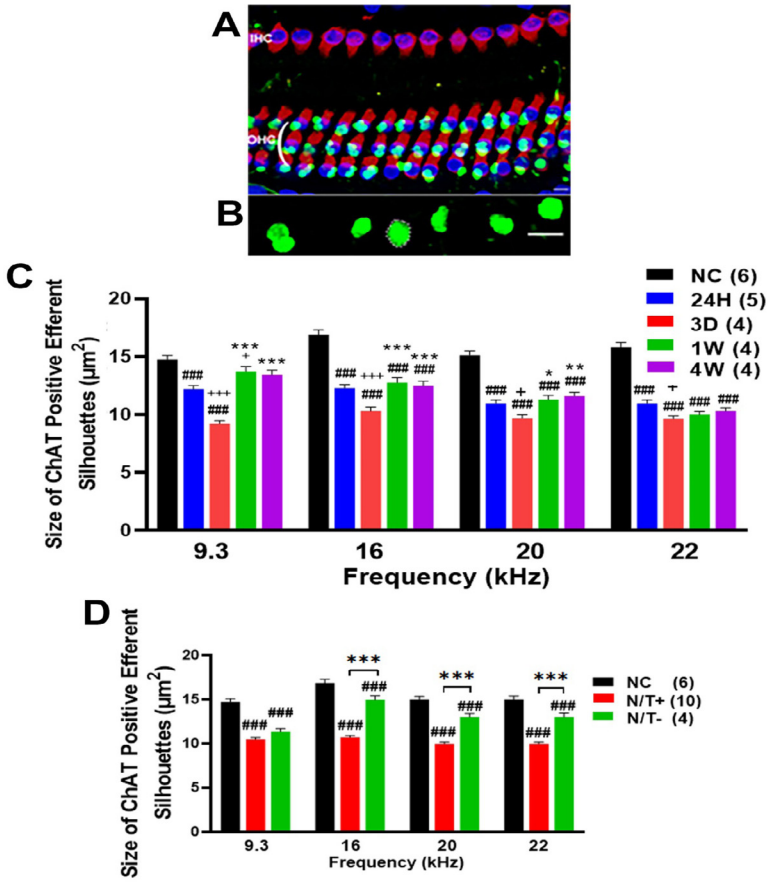

Figure 5: Representative confocal images of OHC efferent termini and their size measurement. A. ChAT immunolabeling (green) was used to demarcate efferent termini on OHCs for subsequent silhouette area measurements. Myosin VIIa immunolabeling identified IHCs and OHCs (red). Nuclei were stained with DAPI (blue). B. Dashed line in B delineates a representative silhouette area used for quantification. Scale bars in A and B = 5 μm. C. Time course of reduced OHC efferent (ChAT) silhouette area sizes post-TTS. OHC ChAT silhouette areas were measured in the ears from NE rats at 24h, 3d, 1w, and 4w post-noise. The size of ChAT silhouette areas was significantly and rapidly (i.e. 24 hours after noise exposure, blue bars) reduced and remained chronically reduced across a broad tonotopic frequency range out to 4 weeks (purple bars) post-noise in comparison to naïve controls (NCs, black bars). ### indicates $p < 0.001$ compared to normal controls, +, +++ indicate $p < 0.05$, < 0.001 compared to 24 hours, *, **, *** indicate $p < 0.05$, < 0.01, < 0.001 compared to 3 days, respectively. D. Evaluation of efferent (ChAT) silhouette areas in rats with or without tinnitus at 4 weeks after TTS. Average silhouette areas were significantly reduced at 4 weeks after noise exposure in the N/T+ group or the N/T- group compared to naïve controls (NC) at tonotopic positions of 9.3, 16, 20 and 22 kHz (###, all $p < 0.001$). Rats with tinnitus had significantly smaller OHC ChAT silhouettes compared to rats without tinnitus (***, all $p < 0.001$) at tonotopic positions of 16, 20, and 22 kHz.

Up-regulation of VR1 and T22 in the spiral ganglion of the TTS model

To explore molecular mechanisms of tinnitus in the peripheral auditory system, we measured VR1 and T22 positive cell densities in the spiral ganglion of rats with tinnitus. Four weeks after noise exposure, significantly more VR1-positive cells were found in the spiral ganglion of all NE rat (all $p < 0.001$). However, there was no significant difference in VR1-positive cell density between the N/T+ and the N/T- groups ($p > 0.05$, **Figure 6A**), indicating up-regulation of VR1 was noise-related only.

Four weeks after noise exposure, significantly more T22 positive cells were found in the spiral ganglion of the N/T+ group compared to the NC group ($p < 0.001$). Although more T22 positive cells were also found in the spiral ganglion of the N/T- group, the difference is not statistically significant compared to the NC group ($p > 0.05$). Furthermore, no significant difference was detected in T22 positive cell density between the N/T+ and the N/T- groups ($p > 0.05$, **Figure 6B**).

Noise-induced biomarker changes in the central auditory system and in the hippocampus Up-regulation of $GABA_AR$-α1 in the central auditory system of the TTS model

To explore neurotransmitter mechanisms of tinnitus in the central auditory system, we measured $GABA_AR$-α1 positive cell density in the DCN and the AC, as well as in the hippocampus of rats 4 weeks post-noise exposure. Numerous $GABA_AR$-α1-positive cells were observed in the DCN of rats from all test cohorts, especially in the DCN of all NE rats (**Figure 7B and C**). Positive cells with different sizes and shapes were located mainly in the fusiform cell layer and the deep layer of the DCN. Significantly more $GABA_AR$-α1 positive cells were observed across all regions (lateral, middle and medial regions) of the DCN of the N/T- group ($p < 0.01$ or 0.001) while only the middle regions of the DCN of the N/T+ group had significantly more $GABA_AR$-α1 positive cells compared to the NC group ($p < 0.05$, **Figure 7D**). The N/T- group had significantly more $GABA_AR$-α1 positive cells in the medial and middle regions of the DCN compared to the N/T+ group (all $p < 0.05$, **Figure 7D**). When the data in **Figure 7** was combined together, we found that all NE rats had significantly more $GABA_AR$-α1-positive cells compared to the NC group ($p < 0.01$ or 0.001). The N/T- group had significantly more $GABA_AR$-α1-positive cells in the DCN than the N/T+ group ($P < 0.001$, **Figure 7E**), suggesting changes in the expression of GABAAR-α1 in the DCN may be tinnitus-related.

In the AC, significantly more $GABA_AR$-α1 positive cells were found in all NE rats compared to the NC group (all $p < 0.001$). However, there was no significant difference in $GABA_AR$-α1-positive cell density between the N/T+ and the N/T- groups ($p > 0.05$), indicating that changes in $GABA_AR$-α1 in the AC are noise-related only. In the PoDG, no change was found in the numbers of $GABA_AR$-α1-positive cells in all NE rats compared to the NC group (all $p > 0.05$, data not shown **Figure 8**).

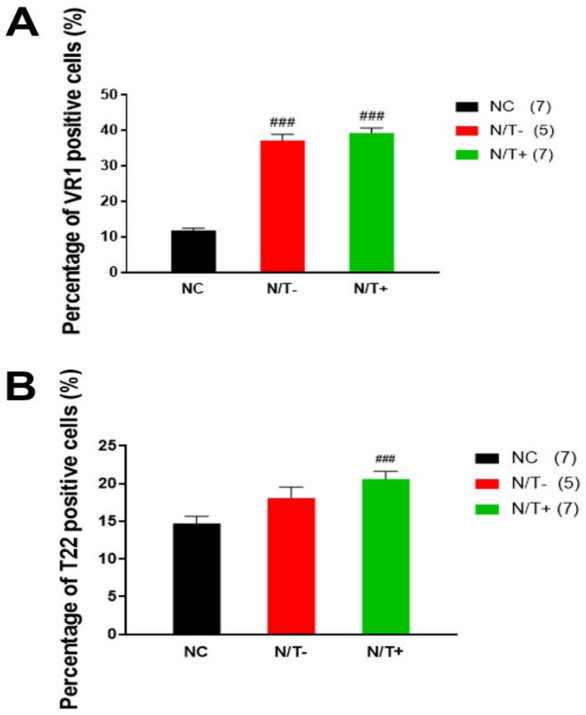

Figure 6: Quantification of VR1 or T22 positive cells in the spiral ganglion 4 weeks after noise exposure. A. Significantly more VR1 positive cells were found in the spiral ganglion of all NE rats (N/T- and N/T+) compared to the NC group (all $p < 0.001$). However, there is no significant difference between the N/T+ and the N/T- groups ($p > 0.05$). B. Significantly more T22 positive cells were found in the spiral ganglion of the N/T+ group compared to the NC group ($p < 0.001$). However, there is no significant difference in T22 positive cell density between the N/T+ and N/T- groups ($p > 0.05$). ### indicate $p < 0.001$ compared to the NC group.

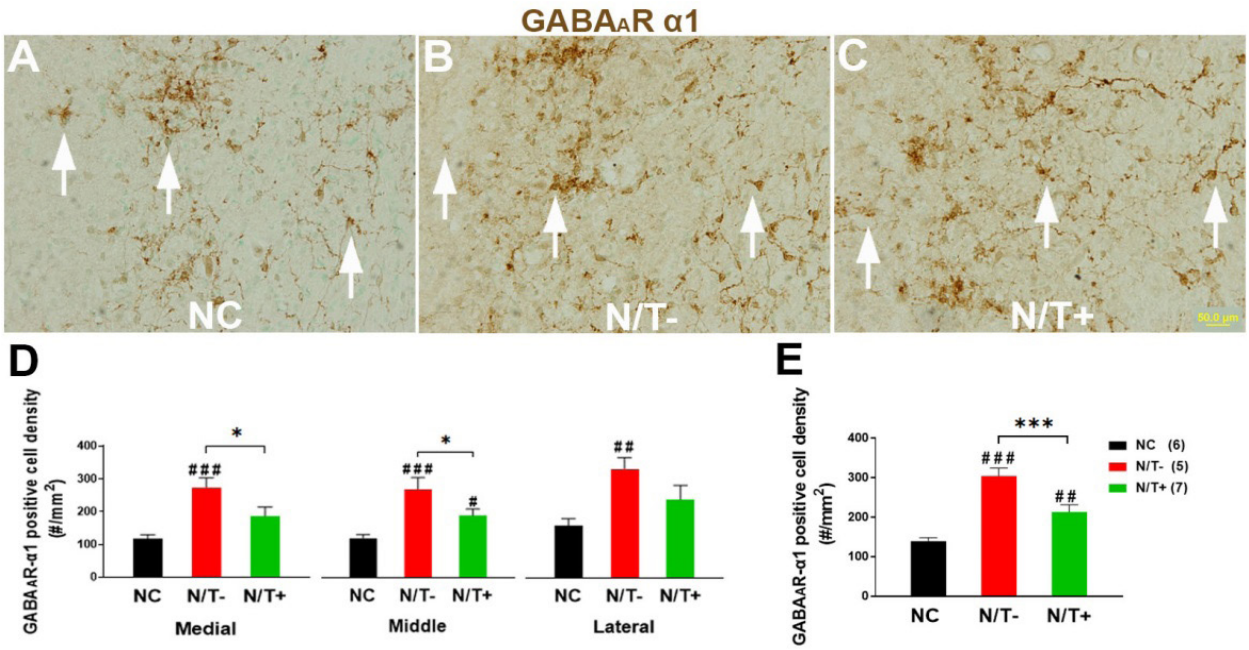

Figure 7: Examples of $GABA_A$R-α1 immunostaining and quantification in the DCN of rats. Numerous $GABA_A$R-α1 positive cells were observed in the DCN of rats of all conditions (A-C), especially in the DCN of NE rats (arrows in B and C). The positive cells had different sizes and shapes (arrows in A-C). Compared to NC, there are significantly more $GABA_A$R-α1 positive cells in the DCN of the N/T- group across all regions (medial, middle and lateral) of the DCN ($p < 0.01$ or 0.001) while only the middle regions of the DCN of the N/T+ group had significantly more $GABA_A$R-α1 positive cells ($p < 0.05$, D). The N/T- group had significantly more $GABA_A$Rα1 positive cells in the medial and middle regions of the DCN compared to the N/T+ group (all $p < 0.05$). Combining the data in D together, all NE rats (N/T- and N/T+) had significantly more $GABA_A$R-α1 positive cells compared to the NC group ($p < 0.01$ or 0.001). The N/T- group had significantly more $GABA_A$R-α1 positive cells than the N/T+ group ($p < 0.001$). #, ## and ### indicate $p < 0.05$, 0.01 and 0,001 compared to the NC group while * and *** indicate $p < 0.05$ and 0.001 compared to rats with tinnitus. Scale bar in C = 50 µm for A-C.

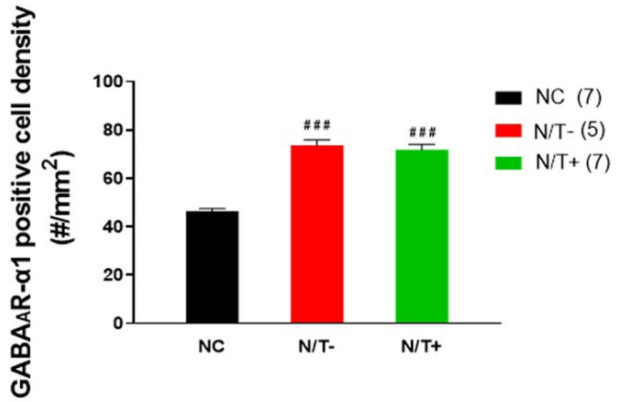

Figure 8: Quantification of $GABA_A$R-α1 positive cells in the AC. All NE rats (N/T- and N/T+) had significantly more $GABA_A$R-α1 positive cells in the AC compared to the NC group (all $p < 0.001$). There is no significant difference in $GABA_A$R-α1 positive cell density in the AC between the N/T+ and the N/T- group (all $p > 0.05$). ### indicate $p < 0.001$ compared to the NC group.

Up-regulation of GluR2 in the central auditory system and in the hippocampus of the TTS model

To explore neurotransmitter mechanisms of tinnitus in the central auditory system, we measured the GluR2 positive cell density in the DCN and the AC, as well as in the hippocampus of rats 4 weeks post-noise exposure. No changes in GluR2 immunostaining were observed in the DCN 4 weeks after noise exposure (all $p > 0.05$, data not shown). GluR2-positive cell density was also not changed in the AC of the N/T- group compared to NCs, however, significantly more GluR2-positive cells were observed in the AC of the N/T+ group compared to the N/T- group ($p < 0.001$, **Figure 9A**). In the PoDG, significantly more GluR2-positive cells were observed in all NE rats compared to the NC group ($p < 0.05$ or 0.001), while the N/T+ group had significantly more GluR2-positive cells compared to the N/T- group ($p < 0.01$, **Figure 9B**). Taken together, these results seem to indicate that changes in GluR2 expression in the AC and in the PoDG are tinnitus-related.

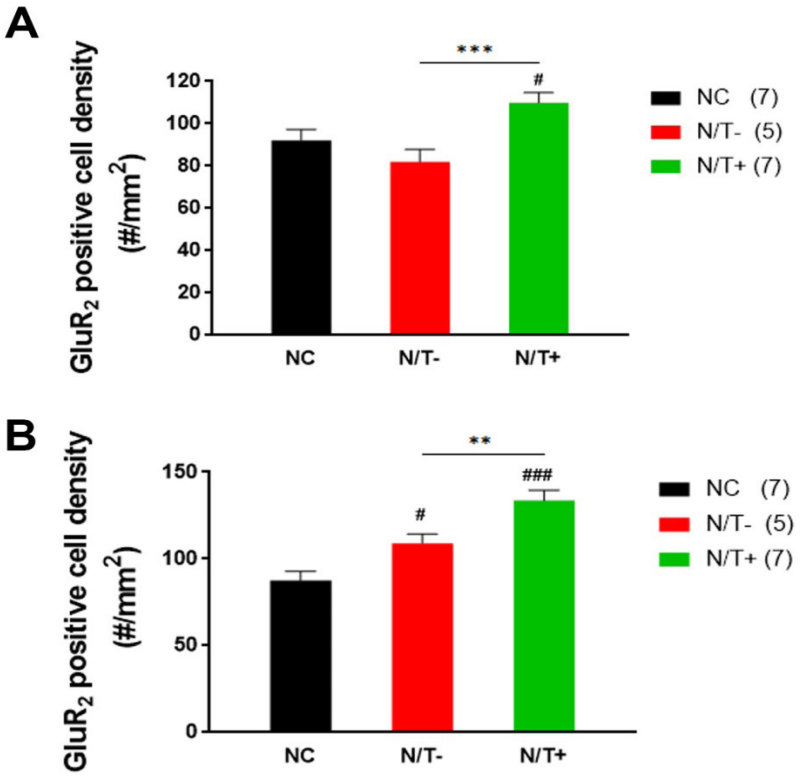

Figure 9: Quantification of GluR2 positive cells in the AC (A) and in the PoDG (B). A. Significantly more GluR2 positive cells were observed in the AC of the N/T+ group compared to the NC group ($p < 0.05$) and the N/T- group ($p < 0.001$). B. Significantly more GluR2 positive cells were observed in the PoDG of all NE rats (N/T- and N/T+) compared to the NC group ($p < 0.05$ or 0.001). The N/T+ group had significantly more GluR2 positive cells than the N/T- group ($p < 0.01$). #, ### indicate $p < 0.05$ or < 0.001 compared to the NC group while ** and *** indicate $p < 0.01$ and 0.001 compared to rats without tinnitus (N/T-).

Up-regulation of T22 in the central auditory system of the TTS model

To explore the potential role of neural degeneration in tinnitus, T22 expression was also examined in the central auditory system and in the hippocampus of rats 4 weeks post-noise exposure. Significantly more T22-positive cells were observed in the DCN of all NE rats compared to the NC group (all $p < 0.001$, **Figure 10**). However, there was no significant difference in T22-positive cell density between the N/T+ and the N/T- groups ($P > 0.05$, **Figure 10**), indicating changes in T22 expression in the DCN are noise-related only. No significant changes were observed in T22-positive cell densities in the AC and in the PoDG of all NE rats compared to the NC group (all $p > 0.05$, data not shown).

Expression of CNS biomarkers after noise exposure is linked to tinnitus

To explore central neural mechanisms underlying tinnitus, $GABA_AR\alpha1$, GluR2 and T22 were monitored as biomarkers in the PoDG, the DCN and the AC, where the number of positive immunostained cells was counted per mm^2 of area as a neural correlate of tinnitus. In total, 18 rats were used for this immunohistochemical staining to gather data at 4 weeks after noise exposure. Of these animals, 6 were from the naïve control group, and 12 were from the noise-exposed group, in which 7 exhibited a tinnitus percept while 5 did not. Here, we sought a correlation between the presence of a tinnitus percept and the expression level of biomarkers in the CNS by including behavioral PPI performance and immunohistochemical measurement in an animal-by-animal study. The Pearson correlation coefficient (r) was calculated to test for the association, while the bootstrapping approach was employed to run hypothesis testing, where bootstrap replicates were set to 2000. Correlation coefficients after Pearson and four different types of CIs after bootstrap (i.e., first order normal approximation or Normal, basic bootstrap interval or Basic, percentile bootstrap interval or Percentile, and bias-corrected and accelerated bootstrap interval or BCa) are listed in (**Table 1**). The Pearson's r between the number of GluR2+ cells per mm2 and the strength of tinnitus perception (expressed in tinnitus index scores) was 0.6993 and 0.4448, respectively for the PoDG and the AC, meaning that the two variables of interest were positively correlated with a large or medium effect size. Here, the 95% CIs for a population correlation coefficient (all 4 bootstrapped CIs for the PoDG; both normal and basic CIs for the AC) did not cross zero, proving statistical significance.

DISCUSSION

In the current study, we have successfully developed a unique rodent NIT animal model. Unlike most tinnitus animal models reported in literature, rats in our study had

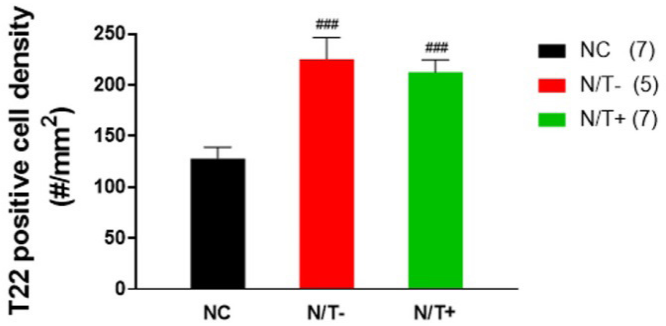

Figure 10: Quantification of T22 positive cells in the DCN of rats. Significantly more T22 positive cells were observed in the DCN of all NE rats (N/T- and N/T+) compared to the NC group (all $p < 0.001$). However, there is no significant difference in T22 positive cell density I the DCN between the N/T+ and the N/T- group ($P > 0.05$). ### indicate $p < 0.001$ compared to the NC group.

Table 1: Correlation of CNS biomarkers with the presence of a tinnitus percept analyzed 4 weeks following noise exposure.

CNS region	Biomarker	Pearson's r	95% CI for a correlation coefficient			
			Normal	Basic	Percentile	BCa
AC	GluR2	0.4448	(0.0267, 0.9236)*	(0.1153, 0.9910)*	(-0.1013, 0.7744)	(-0.1085, 0.7672)
	T22	-0.3247	(-0.8130, 0.2182)	(-0.8198, 0.1703)	(-0.8198, 0.1703)	(-0.7609, 0.3071)
	$GABA_AR$-α1	0.0319	(-0.4124, 0.4836)	(-0.3964, 0.4920)	(-0.4281, 0.4603)	(-0.4046, 0.4719)
PoDG	GluR2	0.6993	(0.4730, 0.9524)*	(0.5296, 1.0171)*	(0.3815, 0.8690)*	(0.3863, 0.8704)*
	T22	-0.3712	(-0.6975, -0.0276)*	(-0.7132, -0.0380)*	(-0.7044, -0.0293)*	(-0.6896, 0.0014)
	$GABA_AR$-α1	-0.287	(-0.6948, 0.1215)	(-0.7076, 0.0896)	(-0.6636, 0.1336)	(-0.6522, 0.1570)
DCN	GluR2	-0.1826	(-0.6274, 0.2218)	(-0.6642, 0.1836)	(-0.5488, 0.2989)	(-0.5734, 0.2552)
	T22	0.3131	(-0.1108, 0.7260)	(-0.1014, 0.7396)	(-0.1133, 0.7276)	(-0.1772, 0.6950)
	$GABA_AR$-α1	-0.2107	(-0.5315, 0.1009)	(-0.5459, 0.0902)	(-0.5117, 0.1244)	(-0.4841, 0.1749)

Note: 1. Correlation coefficients between tinnitus index scores and positive immunostained cell numbers per mm2 area after Pearson, and four types of CIs after bootstrap. 2. * indicates 95% CIs not crossing zero, proving significance. 3. Normal stands for first order normal approximation; Basic for basic bootstrap interval; Percentile for percentile bootstrap interval; BCa for bias-corrected and accelerated bootstrap interval; AC for the auditory cortex; PoDG for the polymorph layer of the dentate gyrus; DCN for the dorsal cochlear nucleus.

very low levels of PTS and no HC loss in the cochlea four weeks after noise exposure. Sixty-seven percent of rats in the present study demonstrated behavioral evidence of tinnitus. This NIT animal model provides a unique opportunity to study the functional consequences of reduced efferent signaling and tinnitus-related biomarker expression in the auditory system on the development and specification of a chronic tinnitus percept without confounding variables.

Consistent with our results, previous animal studies have shown that noise exposures that induce TTS alone can, nonetheless, cause permanent IHC synaptic ribbons loss in the high frequency regions in DBA/CaJ mice[39]. While this RS loss has little effect on hearing thresholds in quiet, it degrades hearing in noisy environments and may be an important contributor to tinnitus development[43]. A unifying "central gain" model of tinnitus has proposed that tinnitus results from a compensatory increase in gain (or sensitivity) at virtually all levels in the central auditory system to compensate for loss of afferent input from the cochlea[11, 44-46]. In fact, previous studies demonstrated that IHC RS loss is correlated with tinnitus development in animals with low levels of permanent hearing loss after noise exposure[10, 47, 48]. Loss of IHC RS is also critical to the development of chronal salicylate sodium-induced tinnitus in rats without hearing loss[49]. In the present study, we did see more RS loss in rats with tinnitus at 32 kHz compared to rats without tinnitus **(Figure 4B)** however,

the difference is not significant. Further investigation would be needed to clarify why RS loss was not more obviously associated with tinnitus in our TTS model.

The primary functions of the auditory efferent system include noise protection, mediation of selective attention, and improvement of noise/signal ratio[18]. Recent clinical evidence suggests that the efferent system, especially the medial efferent system, may be also involved in tinnitus generation and maintenance[20-23]. This involvement may be located at the brainstem level as initially suggested by Hazel and Jastreboff [50]. However, in the current study, we have found for the first time that the size of efferent nerve endings under OHCs, examined by ChaT labeling, was significantly reduced in rats with NIT compared to rats without tinnitus. Our observation indicates that the medial efferent system at the cochlear level is also involved in tinnitus generation and maintenance. However, the functional status of the efferent system has not been examined in this tinnitus animal model, which should be evaluated in the future.

In normal conditions, VR1 enhances background neural activity of spiral ganglion neurons[51]. In pathological conditions, its up-regulation may promote ganglion neuron survival and is involved in neuroplasticity in the cochlea that leads to tinnitus and hyperacusis[52, 53]. Consistent with previous studies[37, 52], significant up-regulation of VR1 was observed in the spiral ganglion of all NE rats four weeks post-noise exposure. However, no difference was observed between rats (**Figure 6A**) with and without tinnitus, suggesting VR1 expression may be not involved in tinnitus-induced by noise exposure although its activation is related to salicylate-induced tinnitus[54]. The role of pathologic Tau in tinnitus development is still unclear. In our model, significantly more T22-positive cells were observed in the spiral ganglion of NE rats with tinnitus, however, no significant difference was observed between rats with and without tinnitus (Figure 6A). Similar results were also found in the DCN of all NE rats **(Figure 10)**. These results suggest that pathologic Tau expression in the spiral ganglion and in the DCN may be a pervasive noise-induced histopathological response that may not be directly involved in tinnitus development. It is, perhaps, noteworthy that elevated serum levels of neurotrauma biomarkers, including Tau, have been reported in military and law enforcement personnel exposed to low-level shock waves during training and in combat, however, only Amyloid β-42 levels were positively associated with tinnitus[55].

Consistent with our previous study[37], significantly more GABA^{A}R-α1 positive cells were observed in the DCN of all NE rats with or without tinnitus four weeks post-noise exposure. However, rats with tinnitus had significantly fewer GABA$_A$R-α1 positive cells in the DCN compared to rats without tinnitus. These results suggest that GABA$_A$R-α1 up-regulation may represent a neuroplastic event to balance the increased excitability in the DCN after injuries[56], and failure of maintaining a high level of GABA$_A$R-α1 in the DCN leads to tinnitus development. However, no changes were observed in the number of GluR2 positive cells in the DCN 4 weeks after noise exposure in the current study. In one of our previous studies, more GluR2 positive cells in the DCN were also observed in the DCN of rats with PTS 9 weeks after blast exposure[37], suggesting the noise level we used in the current study may be relatively too low to induce up-regulation of GluR2 in the DCN. Another possibility is redistribution of synaptic AMPA receptors at glutamatergic synapses in the DCN after insults[57]. Therefore, other AMPA receptor subunits, i.e. GluR2/3, should be included in future similar studies.

In the current study, we have observed significant differences in some biomarkers' expression in the brain and in the cochlea between rats with and without tinnitus. For example, significantly lower expression of GABA$_A$R-α1 was observed in the DCN of rats with tinnitus **(Figure 7)**. Significantly higher expression of GluR2 was observed in the AC and in the PoDG **(Figure 9)**, and up-regulation of T22 was observed in the spiral ganglion of rats with tinnitus **(Figure 6B)**. In the cochlea, significantly smaller OHC efferent termini labelled with ChAT were also observed in rats with tinnitus **(Figure 5)**. We consider that GABA$_A$R-α1 in the DCN, GluR2 in the AC and in the PoDG, T22 in the spiral ganglion and ChAT in the cochlea are tinnitus-related biomarkers. Some biomarkers' expression was up-regulated after noise exposure, however, no significant difference is observed between rats with and without tinnitus (**Figure 7**). For example, up-regulation of T22 in the DCN and VR1 in the spiral ganglion was observed in all NE rats with or without tinnitus. We consider that T22 in the DCN and VR1 in the spiral ganglion are noise-related biomarkers. Up-regulation of T22 and VR1 was also observed in the cochlea or in the brain in our blast-induced hearing loss and traumatic brain injury animal models[38, 58]. It is surprising to see a significant accumulation of T22 in the spiral ganglion and in the DCN after the relatively low intensity of acoustic trauma used in the present study. More studies are needed to further explore the roles of pathologic Tau in noise- or blast-induced hearing loss and tinnitus in the future.

We also did correlation analyses between biomarkers and tinnitus score in the current study. A strong significantly positive correlation was found between tinnitus score and number of GluR2 positive cells in the PoDG of the hippocampus (Pearson's r = 0.6993), (**Table 1**). These results may provide evidence to some extent that glutamate-mediated excitotoxicity in the CNS is linked to NIT, which would support the tinnitus-related central gain enhancement theory. Consistent with our results, previous studies demonstrated that noise exposure changed the balance of excitation and inhibition in the hippocampus. Glutamate concentration was increased while GABA concentration was decreased in the hippocampus after noise exposure[59-61]. The density of vesicular glutamate transporter (VGLUT-1/2) was increased while Vesicular GABA Transporter (VGAT) was decreased in the

hippocampus 2 weeks after noise exposure[62]. Noise exposure also impairs hippocampal neurogenesis[63-65]. Evidence from animal and human studies suggests that the hippocampus and parahippocampal gyrus facilitate maintenance of the memory of tinnitus percept[66]. Also, of note, we found a significant negative relationship between the tinnitus behavioral model and T22+ cell count data in the PoDG ($r = -0.3712$; values of normal, basic and percentile CIs < 0, **Table 1**). However, it is unclear how Tau pathology may progress in subjects with noise-related tinnitus perception, and further work is necessary to define the process. In the DCN, as opposed to the findings in the PoDG and the AC, that same expression monitoring was not found to be correlated with tinnitus behavior.

In summary, we have developed a unique rodent model of chronic noise-induced tinnitus that can be used to aid in identifying the underlying mechanisms of chronic tinnitus induction and maintenance in the absence of other confounding histopathological outcomes and for the development of pharmaceutical treatments for addressing this disorder.

ACKNOWLEDGMENTS

This research was supported by The Oklahoma Center for the Advancement of Science and Technology (OCAST) grant # AR20-014.

REFERENCES

1. Kreuzer PM, Landgrebe M, Schecklmann M, Staudinger S, Langguth B. Trauma-associated tinnitus: audiological, demographic and clinical characteristics. PLoS One 2012;7(9):e45599.
2. Atik A. Pathophysiology and treatment of tinnitus: an elusive disease. Indian J Otolaryngol Head Neck Surg. 2014;66:1-5.
3. Yankaskas K. Prelude: noise-induced tinnitus and hearing loss in the military. Hear Res. 2013;295:3-8.
4. Bhatt JM, Lin HW, Bhattacharyya N. Prevalence, severity, exposures, and treatment patterns of tinnitus in the United States. JAMA Otolaryngol Head Neck Surg. 2016;142(10):959-65.
5. Masterson EA, Themann CL, Luckhaupt SE, Li J, Calvert GM. Hearing difficulty and tinnitus among US workers and non-workers in 2007. Am J Ind Med. 2016;59(4):290-300.
6. Batts S, Stankovic KM. Tinnitus prevalence, associated characteristics, and related healthcare use in the United States: a population-level analysis. Lancet Public Health. 2024;29.
7. Hickox AE, Liberman MC. Is noise-induced cochlear neuropathy key to the generation of hyperacusis or tinnitus?. J Neurophysiol. 2014;111(3):552-64.
8. Knipper M, Van Dijk P, Nunes I, Rüttiger L, Zimmermann U. Advances in the neurobiology of hearing disorders: recent developments regarding the basis of tinnitus and hyperacusis. Prog Neurobiol. 2013;111:17-33.
9. Plack CJ, Barker D, Prendergast G. Perceptual consequences of “hidden” hearing loss. Trends Hear. 2014;18:2331216514550621.
10. Rüttiger L, Singer W, Panford-Walsh R, Matsumoto M, Lee SC, Zuccotti A, et al. The reduced cochlear output and the failure to adapt the central auditory response causes tinnitus in noise exposed rats. PLoS One. 2013;8(3):e57247.
11. Schaette R, McAlpine D. Tinnitus with a normal audiogram: physiological evidence for hidden hearing loss and computational model. J Neurosci. 2011;31(38):13452-7.
12. Liberman MC, Kujawa SG. Cochlear synaptopathy in acquired sensorineural hearing loss: Manifestations and mechanisms. Hear Res. 2017;349:138-47.
13. Liberman MC. Noise-induced and age-related hearing loss: new perspectives and potential therapies. Faculty of 1000. 2017;6:927.
14. Chéry-Croze S, Collet L, Morgon A. Medial olivo-cochlear system and tinnitus. Acta Otolaryngol. 1993;113(3):285-90.
15. Chery-Croze S, Truy E, Morgon A. Contralateral suppression of transiently evoked otoacoustic emissions and tinnitus. Brit J Audiol. 1994;28(4-5):255-66.
16. Attias J, Zwecker-Lazar I, Nageris B, Keren O, Groswasser Z. Dysfunction of the auditory efferent system in patients with traumatic brain injuries with tinnitus and hyperacusis. J Basic Clin Physiol Pharmacol. 2005;16(2-3):117-26.
17. Geven LI, Wit HP, de Kleine E, van Dijk P. Wavelet analysis demonstrates no abnormality in contralateral suppression of otoacoustic emissions in tinnitus patients. Hear Res. 2012;286(1-2):30-40.
18. Ciuman RR. The efferent system or olivocochlear function bundle–fine regulator and protector of hearing perception. Int J Biol Sci. 2010;6(4):276.
19. Guinan Jr JJ. Olivocochlear efferents: Their action, effects, measurement and uses, and the impact of the new conception of cochlear mechanical responses. Hear Res. 2018;362:38-47.
20. Attias J, Bresloff I, Furman V. The influence of the efferent auditory system on otoacoustic emissions in noise induced tinnitus: clinical relevance. Acta Otolaryngol. 1996;116(4):534-9.
21. Prasher D, Ceranic B, Sulkowski W, Guzek W. Objective evidence for tinnitus from spontaneous emission variability. Noise & Health. 2001;3(12):61-73.
22. Veuillet E, Khalfa S, Collet L. Clinical relevance of medial efferent auditory pathways. Scandinavian Audiology. Supplementum. 1999;51:53-62.
23. Xu J, Liu C, Guo L, Lian N, Liu B. Spontaneous otoacoustic emissions and efferent control of cochlea. Zhonghua Er Bi Yan Hou Tou Jing Wai Ke Za Zhi. 2001;36(6):436-40.
24. Brozoski TJ, Spires TJ, Bauer CA. Vigabatrin, a GABA transaminase inhibitor, reversibly eliminates tinnitus in an animal model. J Assoc Res Otolaryngol. 2007;8:105-18.
25. Balaram P, Hackett TA, Polley DB. Synergistic transcriptional changes in AMPA and GABAA receptor genes support compensatory plasticity following unilateral hearing loss. Neurosci J. 2019;407:108-19.
26. Sarro EC, Kotak VC, Sanes DH, Aoki C. Hearing loss alters the subcellular distribution of presynaptic GAD and postsynaptic GABAA receptors in the auditory cortex. Cereb Cortex. 2008;18(12):2855-67.

27. Middleton JW, Kiritani T, Pedersen C, Turner JG, Shepherd GM, Tzounopoulos T. Mice with behavioral evidence of tinnitus exhibit dorsal cochlear nucleus hyperactivity because of decreased GABAergic inhibition. Proc Natl Acad Sci. 108(18):7601-6.

28. Wang H, Brozoski TJ, Turner JG, Ling L, Parrish JL, Hughes LF, et al. Plasticity at glycinergic synapses in dorsal cochlear nucleus of rats with behavioral evidence of tinnitus. Neurosci. 164(2):747-59.

29. Langguth B, Elgoyhen AB, Cederroth CR. Therapeutic approaches to the treatment of tinnitus. Annu Rev Pharmacol Toxicol. 59(1):291-313.

30. Brozoski T, Odintsov B, Bauer C. Gamma-aminobutyric acid and glutamic acid levels in the auditory pathway of rats with chronic tinnitus: a direct determination using high resolution point-resolved proton magnetic resonance spectroscopy (1H-MRS). Front Syst Neurosci.6:9.

31. Imsuwansri T, Hoare DJ, Phaisaltuntiwongs W, Srisubat A, Snidvongs K. Glutamate receptor antagonists for tinnitus. Cochrane Database Syst Rev. 2016;2016(10).

32. Wang K, Tang D, Ma J, Sun S. Auditory neural plasticity in tinnitus mechanisms and management. Neural Plast. 2020;2020(1):7438461.

33. Gardner SM, Trussell LO, Oertel D. Correlation of AMPA receptor subunit composition with synaptic input in the mammalian cochlear nuclei. Neurosci J. 2001;21(18):7428-37.

34. Wu C, Wu X, Yi B, Cui M, Wang X, Wang Q, et al. Changes in GABA and glutamate receptors on auditory cortical excitatory neurons in a rat model of salicylate-induced tinnitus. Am J Transl Res. 2018;10(12):3941.

35. Isler B, Von Burg N, Kleinjung T, Meyer M, Stämpfli P, Zölch N, et al. Lower glutamate and GABA levels in auditory cortex of tinnitus patients: a 2D-JPRESS MR spectroscopy study. Sci Rep. 2022;12(1):4068.

36. McGill M, Hight AE, Watanabe YL, Parthasarathy A, Cai D, Clayton K, et al. Neural signatures of auditory hypersensitivity following acoustic trauma. Elife. 2022;11:e80015.

37. Lu J, West MB, Du X, Cai Q, Ewert DL, Cheng W, et al. Electrophysiological assessment and pharmacological treatment of blast-induced tinnitus. PLoS One. 2021;16(1):e0243903.

38. Du X, West MB, Cai Q, Cheng W, Ewert DL, Li W, et al. Antioxidants reduce neurodegeneration and accumulation of pathologic Tau proteins in the auditory system after blast exposure. Free Radic Biol Med. 2017;108:627-43.

39. Kujawa SG, Liberman MC. Adding insult to injury: cochlear nerve degeneration after “temporary” noise-induced hearing loss. J Neurosci. 2009;29(45):14077-85.

40. Du X, Ewert DL, Cheng W, West MB, Lu J, Li W, et al. Effects of antioxidant treatment on blast-induced brain injury. PloS one. 2013;8(11):e80138.

41. Du X, Chen K, Choi CH, Li W, Cheng W, Stewart C, et al. Selective degeneration of synapses in the dorsal cochlear nucleus of chinchilla following acoustic trauma and effects of antioxidant treatment. Hear Res. 2012;283(1-2):1-3.

42. Idrizbegovic E, Bogdanovic N, Canlon B. Modulating calbindin and parvalbumin immunoreactivity in the cochlear nucleus by moderate noise exposure in mice.: a quantitative study on the dorsal and posteroventral cochlear nucleus. Brain Res. 1998;800(1):86-96.

43. Hickman TT, Smalt C, Bobrow J, Quatieri T, Liberman MC. Blast-induced cochlear synaptopathy in chinchillas. Sci Rep. 2018;8(1):10740.

44. McGill M, Hight AE, Watanabe YL, Parthasarathy A, Cai D, Clayton K, et al. Neural signatures of auditory hypersensitivity following acoustic trauma. Elife. 2022;11:e80015.

45. Noreña AJ. An integrative model of tinnitus based on a central gain controlling neural sensitivity. Neurosci Biobehav Rev. 2011;35(5):1089-109.

46. Schaette R, Kempter R. Predicting tinnitus pitch from patients’ audiograms with a computational model for the development of neuronal hyperactivity. J Neurophysiol. 2009;101(6):3042-52.

47. Altschuler RA, Halsey K, Kanicki A, Martin C, Prieskorn D, DeRemer S, et al. Small arms fire-like noise: effects on hearing loss, gap detection and the influence of preventive treatment. Neurosci. 2019;407:32-40.

48. Singer W, Zuccotti A, Jaumann M, Lee SC, Panford-Walsh R, Xiong H, et al. Noise-induced inner hair cell ribbon loss disturbs central arc mobilization: a novel molecular paradigm for understanding tinnitus. Mol Neurobiol. 2013;47:261-79.

49. Zhang W, Peng Z, Yu S, Song QL, Qu TF, He L, et al. Loss of Cochlear Ribbon Synapse Is a Critical Contributor to Chronic Salicylate Sodium Treatment-Induced Tinnitus without Change Hearing Threshold. Neural Plast. 2020;2020(1):3949161.

50. Hazell JW, Jastreboff PJ. Tinnitus. I: Auditory mechanisms: a model for tinnitus and hearing impairment. J Otolaryngol. 1990;19(1):1-5.

51. Zhou J, Balaban C, Durrant JD. Effect of intracochlear perfusion of vanilloids on cochlear neural activity in the guinea pig. Hear Res. 2006;218(1-2):43-9.

52. Bauer CA, Brozoski TJ, Myers KS. Acoustic injury and TRPV1 expression in the cochlear spiral ganglion. Int Tinnitus J. 2007;13(1):21.

53. Kitahara T, Li HS, Balaban CD. Changes in transient receptor potential cation channel superfamily V (TRPV) mRNA expression in the mouse inner ear ganglia after kanamycin challenge. Hear Res. 2005;201(1-2):132-44.

54. Kizawa K, Kitahara T, Horii A, Maekawa C, Kuramasu T, Kawashima T, et al. Behavioral assessment and identification of a molecular marker in a salicylate-induced tinnitus in rats. Neurosci. 2010;165(4):1323-32.

55. Boutté AM, Thangavelu B, Nemes J, LaValle CR, Egnoto M, Carr W, et al. Neurotrauma biomarker levels and adverse symptoms among military and law enforcement personnel exposed to occupational overpressure without diagnosed traumatic brain injury. JAMA Net Open. 2021;4(4):e216445-.

56. Dong S, Mulders WH, Rodger J, Woo S, Robertson D. Acoustic trauma evokes hyperactivity and changes in gene expression in guinea-pig auditory brainstem. Eur J Neurosci. 2010;31(9):1616-28.

57. Rubio ME. Redistribution of synaptic AMPA receptors at glutamatergic synapses in the dorsal cochlear nucleus as an early response to cochlear ablation in rats. Hear Res. 2006; 216:154-67.

58. Du X, West MB, Cheng W, Ewert DL, Li W, Saunders D, et al. Ameliorative Effects of Antioxidants on the Hippocampal Accumulation of Pathologic Tau in a Rat Model of Blast□ Induced Traumatic Brain Injury. Oxid Med Cell Longev. 2016;2016(1):4159357.

59. Cui B, Wu M, She X. Effects of chronic noise exposure on spatial learning and memory of rats in relation to neurotransmitters and NMDAR2B alteration in the hippocampus. J Occup Health. 2009;51(2):152-8.

60. Cui B, Wu M, She X, Liu H. Impulse noise exposure in rats causes cognitive deficits and changes in hippocampal neurotransmitter signaling and tau phosphorylation. Brain Res. 2012;1427:35-43.

61. Bo CU, Wu MQ, Zhu LX, She XJ, Qiang MA, Liu HT. Effect of chronic noise exposure on expression of N-methyl-D-aspartic acid receptor 2B and Tau phosphorylation in hippocampus of rats. Biomed Environ Sci. 2013;26(3):163-8.

62. Zhang L, Wu C, Martel DT, West M, Sutton MA, Shore SE. Noise exposure alters glutamatergic and GABAergic synaptic connectivity in the hippocampus and its relevance to tinnitus. Neural Plast. 2021;2021(1):8833087.

63. Dong Y, Zhou Y, Chu X, Chen S, Chen L, Yang B, et al. Dental noise exposed mice display depressive-like phenotypes. Mol Brain. 2016;9:1-0.

64. Kraus KS, Mitra S, Jimenez Z, Hinduja S, Ding D, Jiang H, et al. Noise trauma impairs neurogenesis in the rat hippocampus. Neurosci. 2010;167(4):1216-26.

65. Liu L, Shen P, He T, Chang Y, Shi L, Tao S, et al. Noise induced hearing loss impairs spatial learning/memory and hippocampal neurogenesis in mice. Sci Rep. 2016;6(1):20374.

66. Berger JI, Billig AJ, Sedley W, Kumar S, Griffiths TD, Gander PE. What is the role of the hippocampus and parahippocampal gyrus in the persistence of tinnitus?. Hum Brain Mapp. 2024;45(3):e26627.